Biochemical Characterization of NotB as an FAD-Dependent Oxidase in the Biosynthesis of Notoamide Indole Alkaloids

6 AUTHORS, INCLUDING:

Shengying Li
Chinese Academy of Sciences
36 PUBLICATIONS   **553** CITATIONS

SEE PROFILE

David H Sherman
University of Michigan
265 PUBLICATIONS   **7,578** CITATIONS

SEE PROFILE

Biochemical Characterization of NotB as an FAD-Dependent Oxidase in the Biosynthesis of the Notoamide Indole Alkaloids

Shengying Li[1], **Jennifer M. Finefield**[2], **James D. Sunderhaus**[2], **Timothy J. McAfoos**[2], **Robert M. Williams**[2,4,*], and **David H. Sherman**[1,3,*]

[1]Life Sciences Institute, University of Michigan, Ann Arbor, Michigan 48109

[2]Department of Chemistry, Colorado State University, Fort Collins, Colorado 80523

[3]Departments of Medicinal Chemistry, Microbiology & Immunology, and Chemistry, University of Michigan, Ann Arbor, Michigan 48109

[4]University of Colorado Cancer Center, Aurora, Colorado 80045, USA

Abstract

Notoamides produced by *Aspergillus* spp. bearing the bicyclo [2.2.2] diazaoctane core structure with unusual structural diversity represent a compelling system to understand the biosynthesis of fungal prenylated indole alkaloids. Herein, we report the *in vitro* characterization of NotB, which catalyzes the indole 2,3-oxidation of notoamide E (**13**), leading to notoamide C (**11**) and D (**12**) through an apparent Pinacol-like rearrangement. This unique enzymatic reaction with high substrate specificity, together with the information derived from the precursor incorporation experiments using $[^{13}C]_2$-$[^{15}N]_2$ quadruply labeled notoamide S (**10**) demonstrates **10** as a pivotal branching point in notoamide biosynthesis.

Keywords

Notoamide; fungi; prenylated indole alkaloids; biosynthesis; FAD monooxygenase

---

The family of fungal prenylated indole alkaloids has attracted considerable interest due to their wide spectrum of biological activities, and serve as fascinating targets for chemical synthesis and biosynthetic studies[1]. Family members include the anticancer agents stephacidin (**1**) and avrainvillamide (**2**), anthelmintic paraherquamide (**3**), calmodulin-inhibitor malbrancheamide (**4**), insecticidal brevianamide (**5**) and sclerotiamides (**6**), tremorgenic mycotoxin fumitremorgin (**7**) (Figure 1), and a growing number of related novel bioactive metabolites[1,2].

The notoamides represent relatively new members of this family of prenylated indole alkaloids[3]. Their structures (Figures 1 and 2) contain the unique bicyclo [2.2.2] diazaoctane core proposed to arise from an intramolecular Diels-Alder (IMDA) reaction, while the spiro-oxindole functionality present in notoamide A (**8**) and B (**9**) is presumably derived from an

epoxide-initiated Pinacol-type rearrangement, and are intriguing with respect to their biosynthetic origin.[4] An additional fascinating element in the biosynthesis of the notoamides and stephacidins is the discovery that the marine-derived *Aspergillus* sp. MF297-2 exclusively produces the enantiomers of (+)-**1**, (−)-**8**, and (−)-**9**, whereas the terrestrial *A. versicolor* NRRL 35600 generates the antipodal products (−)-**1**, (+)-**8**, and (+)-**9**[3c] (Figure 1). This implies the biosynthetic enzymes involved in assembly and tailoring might have evolved to catalyze an "identical" reaction to give an enantiomerically distinct product.

To address these biosynthetic questions, we recently sequenced the genome of *Aspergillus* sp. MF297-2 and identified the 42456 bp notoamide biosynthetic gene cluster (*not*) (GenBank accession number HM622670.1) through *in silico* sequence database mining[5].

Based on deep annotation of the predicted **Not** biosynthetic enzymes, together with previous biomimetic syntheses of postulated biosynthetic intermediates[4,6] and corresponding feeding studies with stable isotopically labeled compounds,[7] a putative major biosynthetic pathway for **1, 8**, and **9** has been proposed by these laboratories (Figure 2). Moreover, *in vitro* characterization of the reverse prenyltransferase NotF and normal prenyltransferase NotC has partially established the early steps of the notoamide pathway leading to notoamide S (**10**)[5] (Figure 2). We recently proposed biosynthetic intermediate **10** to be the likely substrate for the hypothetical Diels Alderase as well as a pivotal branch point in notoamide biosynthesis.[4] Specifically, in this study when ^{13}C (C12 & C18), ^{15}N (N13 & N19) quadruply labeled **10** was administered to cultures of *A. versicolor*, (−)-**1**, (+)-**9**, its diastereomer versicolamide B[3c], together with notoamide C (**11**) and D (**12**) were found to contain significant ^{13}C and ^{15}N isotope incorporation (see Supporting Information). In contrast, earlier precursor incorporation experiments in *Aspergillus* sp. MF297-2 and *A. versicolor* were conducted using doubly ^{13}C-labeled (C12 & C17) notoamide E (**13**) that presumably arises from **10** via an oxidative pyran ring closure, in which ^{13}C incorporation was observed only in **11, 12**, and a novel product 3-*epi*-notoamide C (**14**).[7a] No isotopic enrichment was observed in compounds containing the bicyclo[2.2.2] diazaoctane ring, including **1, 8**, and **9**. These results strongly suggest that **13** does not undergo a biosynthetic IMDA leading to **1**. Thus, the biogenesis of **11**-**14** as well as **1, 8** & **9** is proposed to arise from **10** serving as the common precursor (Figure 2).

To test this hypothesis and further elucidate details of the entire notoamide biosynthetic pathway, we have initiated a biochemical analysis of all Not biosynthetic enzymes. To extend our recent investigation of the two prenyltransferases NotC and NotF,[5] we herein report *in vitro* characterization of NotB, an FAD-dependent monooxygenase (FMO) responsible for converting early intermediate **13** to **12** and **11**, the final products of the major branching pathway.

Previously, the *notB* open reading frame (ORF) was predicted to consist of three exons (3486-4079, 4141-4487, and 4568-4829)[5], based on which this ORF was cloned by PCR amplification using the cDNA template prepared by reverse transcription PCR (RT-PCR) from the total RNA isolated from *Aspergillus* sp MF297-2. Next, the *notB* ORF was sub-cloned into the pET28b vector. However, the heterologous expression of *notB* in *Escherichia coli* BL21 (DE3) and BL21 CodonPlus (DE3)-RIPL cells was unsuccessful, which led to a reconsideration of the *notB* ORF annotation. Careful inspection of the 5′ upstream sequence of the assigned start codon resulted in identification of an additional exon-intron pair. Interestingly, the previous start codon within the new intron is only 4 bp away from the 3′ splicing site (AG-3′) of the newly identified intron, thus explaining why the previous mis-annotation resulted in cloning of the partial *notB* gene using the forward primer that is partially complementary to the second exon. Based on the revised annotation, the new version of the *notB* ORF was cloned into pET28b. Sequencing of this new gene

identified another minor error generated by *in silico* prediction. The predicted exon 3486-4079 was revealed to be 6 bp shorter than the actual sequence due to two close 5′ splicing sites (5′-GT) (see Supporting Information). As a result of these two additional changes, the organization of *notB* exons were again revised to 3265-3433, 3493-4085, 4141-4487, and 4568-4829. Notably, a similar correction of exon organization was also made to *AFUA_6g12060* from *A. fumigatus* Af293[8], an FMO gene homologous to *notB*.

The new construct pET28b-*notB* was successfully expressed in *E. coli* BL21 CodonPlus (DE3)-RIPL strain to generate N-terminal His$_6$-tagged recombinant NotB. The protein was purified to homogeneity by tandem Ni-NTA chromatography. The light yellow NotB solution displayed an ultraviolet-visible absorption spectrum consistent with a flavoprotein. The yellow color retained with the supernatant after boiling and centrifugation to pellet the denatured protein indicated the flavin cofactor is non-covalently bound. Further HPLC analysis of the supernatant clearly showed FAD instead of FMN serves as the NotB cofactor (see Supporting Information). The percent holoprotein was determined to be 90% using the concentration of the released FAD upon denaturation that was calculated from its characteristic absorption at 446 nm *versus* the concentration of purified NotB based on Bradford assay using bovine serum albumin (BSA) as standard.

The *in vitro* activity of NotB against **1, 8, 10, 13**, and a number of other synthetic notoamide pathway intermediates including notoamide T (**15**), brevianamide F, deoxybrevianamide E, and 6-OH-deoxybrevianamide E (see Supporting Information) was tested in the presence of NADH/NADPH. The only reaction observed was for **13**, which generated two products of greater polarity (Figure 3A), both with a molecular weight 16 amu greater than **13**. Co-injection of the synthetic standards of **11, 12**, and **14** with products of the NotB reaction mixture confirmed **12** and **11** (~16:1) as the major and minor oxidative products, respectively. Although a biosynthetic pathway from **13** to **11, 12** and **14** via a non-stereospecific epoxidation and subsequent Pinacol rearrangement was previously proposed[4b], reexamination of spectral data and reasonable biosynthetic priniciples have led us to revise the C3 stereochemistry for previously defined notoamide C (**11**) and *epi*-notoamide C (**12**) (shown in Figure 2; also see Supporting Information). Notably, the *in vitro* NotB reaction did not produce **14**, which has been previously isolated from a precursor incorporation experiment with **13** as an added substrate, but not directly from fermentation extracts of *Aspergillus* sp. MF297-2[7a]. This suggests that **14** might be an artifact arising from excess **13**, or alternatively, **14** might be generated adventitously from an undefined FMO (NotI) that is highly related to NotB in the same gene cluster (see below). Further analysis demonstrated that only NADPH (not NADH) is capable of supporting NotB activity. By monitoring the consumption of substrate, the apparent reaction velocity at 200 μM of **13** was determined to be 34 ± 3 μM/min (see Supporting Information). The steady-state Michaelis-Menton kinetics of NotB could not be ascertained due to significant substrate inhibition and limited aqueous solubility of hydrophobic **13**. However, the apparent specificity constant (k_{cat}/K_m) determined by fitting the lowconcentration (10-80 μM) data to the linear region of the Michaelis-Menten curve was shown to be 8.70 $\mu M^{-1} min^{-1}$ (see Supporting Information).

Previously, the mechanism for generation of **11** and **12** from **13** was proposed to proceed via a non-stereospecific 2,3-epoxidation of the indole followed by Pinacol-type rearrangement (for **11**)[4b] (Figure 4A and Supporting Information). Ring opening of the β-2,3-epoxyindole intermediate (**16a**) to the 3-hydroxyindolenine species **17a**, followed by N-C ring closure from the diketopiperazinyl NH generates pyrroloindole **12** (notoamide D) as the major product. As the minor product, our current data is consistent with **11** being derived from **16a** via the pseudo-*para*-quinone methide species **18a** and subsequent α-face migration of the prenyl group from C2 to C3 to quench the quinone methide (Figure 4A). In contrast, the α-

face epoxide intermediate would lead to β-face migration of the prenyl group resulting in 2-oxindole product **14**. We would expect that the α-face epoxide intermediate **18a** might also generate a diastereomer of **12** (*epi*-notoamide D, see Supporting Information). However, formation of **14** and *epi*-notoamide D was not observed, suggesting that NotB does not catalyze α-face epoxidation. In addition, formation of two sets of diasteromers is inconsistent with the typical high stereoselectivity of natural product biosynthetic enzymes.

Characterization of NotB as the notoamide E oxidase offered an opportunity to address the presumed catalytic mechanism for this unique biotransformation. Since involvement of the diketopiperazinyl N19-H represents a key feature in these alternative routes, we elected to synthesize the substrate analogue **19** (Figure 4A) with the N19 position methylated. Following conversion by NotB, a single oxidative product with observed mass $[M+H]^+ =$ 463.20 (*calc* 463.24, 16 amu greater than m.w. of **13**) was detected by LC-MS analysis (Figure 4C), confirmed to be N19 methylated notoamide C (**20**) by co-injection with the synthesized authentic standard (Figure 4C and Supporting Information). This result clearly indicates that NotB specifies β-epoxidation because an additional isolable product derived from the highly unstable α-epoxide intermediate would otherwise be detected. Mechanistically, when N19 is methylated in **17b**, the ring closure to form **12** is blocked, thus shifting the major pathway (from species **17b** to **12**) to exclusive formation of the oxindole product **20**.

In summary, we have reconstituted NotB from the notoamide biosynthetic pathway, which efficiently and stereoselectively oxidizes **13** with predominant formation of **12** over **11** (~16:1). In contrast, **11** and **14** instead of **12** were shown as major products (76% combined yield) in a previous biomimetic synthesis of **11** and **12** utilizing chemical oxidants.[4b] This difference highlights the ability of NotB to provide greater control over the reaction selectivity than the chemical method. Using the synthetic substrate analogue **19**, the NotB reaction was exclusively directed to formation of notoamide C analogue **20**, indicating a β-face specific oxidative mechanism for NotB (Figure 4B) and the proposed revision to the previous structural assignment for **11** and **14** (see Supporting Information). However, final confirmation of the new mechanism and the structural basis for its β-face stereoselectivity awaits elucidation of the cocrystal structure of NotB with product **11** (or **14**).

The inactivity of NotB toward **10** indicates this enzyme possesses stringent substrate specificity. In addition, the *in vivo* conversion from 6-OH-deoxybrevianamide E to notoamide J via a similar indole 2,3-epoxidation supported by recent labeled precursor incorporation studies[7b] is unlikely due to the activity of NotB since 6-OHdeoxybrevianamide E failed to serve as a substrate for this flavin oxidase *in vitro* (see Supporting Information). However, the possibility that NotB may behave differently *in vivo* from the *in vitro* system cannot be excluded.

Finally, another FMO gene *notI* resides in the notoamide gene cluster, whose protein product (NotI) is highly similar to NotB with 42% protein sequence identity and 59% similarity. Thus, their possible functional and structural similarity and evolutionary relationship is of significant interest. Moreover, the NotB homolog Af12060[8b] (33/48%: *Id/Sim*%) involved in fumiquinazoline biosynthesis in *A. fumigutas* Af293 was found to oxidize the 2,3-double bond of the indole group of fumiquinazoline F, suggesting this might be a general strategy adopted by filamentous fungi to oxidize indole moieties. In contrast, another NotB homolog TqaE[8c] with a closer relationship (45/63%: *Id/Sim*%) in tryptoquialanine biosynthesis in *Penicillium aethiopicum* was recently reported to catalyze *N*-hydroxylation, reflecting a divergently evolved function of this FMO subfamily.

Supplementary Material

Refer to Web version on PubMed Central for supplementary material.

REFERENCES

(1). (a) Williams RM, Stocking EM, Sanz-Cervera JF. Topics Curr. Chem. 2000; 209:97–173.(b) Li S-M. Nat. Prod. Rep. 2010; 27:57–78. [PubMed: 20024094] (c) Li S-M. J. Antibiot. 2011; 64:45–49. [PubMed: 21063425]

(2). (a) Qian-Cutrone J, Huang S, Shu Y-Z, Vyas D, Fairchild C, Menendez A, Krampitz K, Dalterio R, Klohr SE, Gao Q. J. Am. Chem. Soc. 2002; 124:14556–14557. [PubMed: 12465964] (b) Wulff JE, Siegrist R, Myers AG. J. Am. Chem. Soc. 2007; 129:14444–14451. [PubMed: 17958425] (c) Blanchflower SE, Banks RM, Everett JR, Manger BR, Reading CJ. Antibiot. 1991:492–497.(d) Miller KA, Figueroa M, Valente MW, Greshock TJ, Mata R, Williams RM. Bioorg. Med. Chem. Lett. 2008; 18:6479–6481. [PubMed: 18986806] (e) Birch AJ, Wright JJ. Tetrahedron. 1970; 26:2329–2344. [PubMed: 5419195] (f) Paterson RRM, Simmonds MJS, Kemmelmeier C, Blaney WM. Mycol. Res. 1990; 94:538–542.(g) Whyte AC, Gloer JB. J. Nat. Prod. 1996:1093–1095. [PubMed: 8946752]

(3). (a) Kato H, Yoshida T, Tokue T, Nojiri Y, Hirota H, Ohta T, Williams RM, Tsukamoto S. Angew. Chem. Int. Ed. 2007; 46:2254–2256.(b) Tsukamoto S, Kato H, Samizo M, Nojiri Y, Onuki H, Hirota H, Ohta T. J. Nat. Prod. 2008; 71:2064–2067. [PubMed: 19053517] (c) Greshock TJ, Grubbs AW, Jiao P, Wicklow DT, Gloer JB, Williams RM. Angew. Chem. Int. Ed. 2008; 47:3573–3577.(d) Tsukamoto S, Kawabata T, Kato H, Greshock TJ, Hirota H, Ohta T, Williams RM. Org. Lett. 2009; 11:1297–1300. [PubMed: 19281134] (e) Tsukamoto S, Kato H, Greshock TJ, Hirota H, Ohta T, Williams RM. J. Am. Chem. Soc. 2009; 131:3834–3835. [PubMed: 19292484] (f) Tsukamoto S, Umaoka H, Yoshikawa K, Ikeda T, Hirota H. J. Nat. Prod. 2010; 73:1438–1440. [PubMed: 20795742]

(4). (a) Sunderhaus JD, Sherman DH. Isr. J. Chem. 2011; 51:442–452. [PubMed: 21818159] (b) Grubbs AW, Artman GD III, Tsukamoto S, Williams RM. Angew. Chem. Int. Ed. 2007; 46:2257–2261.(c) Greshock TJ, Grubbs AW, Tsukamoto S, Williams RM. Angew. Chem. Int. Ed. 2007; 46:2262–2265.

(5). Ding Y, de Wet JR, Cavalcoli J, Li S, Greshock TJ, Miller KA, Finefield JM, Sunderhaus JD, McAfoos TJ, Tsukamoto S, Williams RM, Sherman DH. J. Am. Chem. Soc. 2010; 132:12733–12740. [PubMed: 20722388]

(6). (a) Finefield JM, Williams RM. J. Org. Chem. 2010; 75:2785–2789. [PubMed: 20359229] (b) McAfoos TJ, Li S, Tsukamoto S, Sherman DH, Williams RM. Heterocycles. 2010; 82:461–472. [PubMed: 21796227] (c) Williams RM, Glinka T, Kwast E, Coffman H, Stille JK. J. Am. Chem. Soc. 1990; 112:808–821.

(7). (a) Tsukamoto S, Kato H, Greshock TJ, Hirota H, Ohta T, Williams RM. J. Am. Chem. Soc. 2009; 131:3834–3835. [PubMed: 19292484] (b) Finefield JM, Sherman DH, Tsukamoto S, Williams RM. J. Org. Chem. 2011; 76:5954–5958. [PubMed: 21504234]

(8). (a) Williams RM, Stocking EM, Sanz-Cervera JF. Top. Curr. Chem. 2000; 209:97–173.(b) Ames BD, Liu X, Walsh CT. Biochemistry. 2010; 49:8564–8576. [PubMed: 20804163] (c) Gao X, Chooi Y-H, Ames BD, Wang P, Walsh CT, Tang Y. J. Am. Chem. Soc. 2011; 133:2729–2741. [PubMed: 21299212] (d) Haynes S, Ames BD, Gao X, Tang Y, Wlsh CT. Biochemistry. 2011; 50:5668–5679. [PubMed: 21591693] (e) Ames BD, Haynes SW, Gao X, Evans BS, Kelleher NL, Tang Y, Walsh CT. Biochemistry. 2011; 50:8756–8769. [PubMed: 21899262]
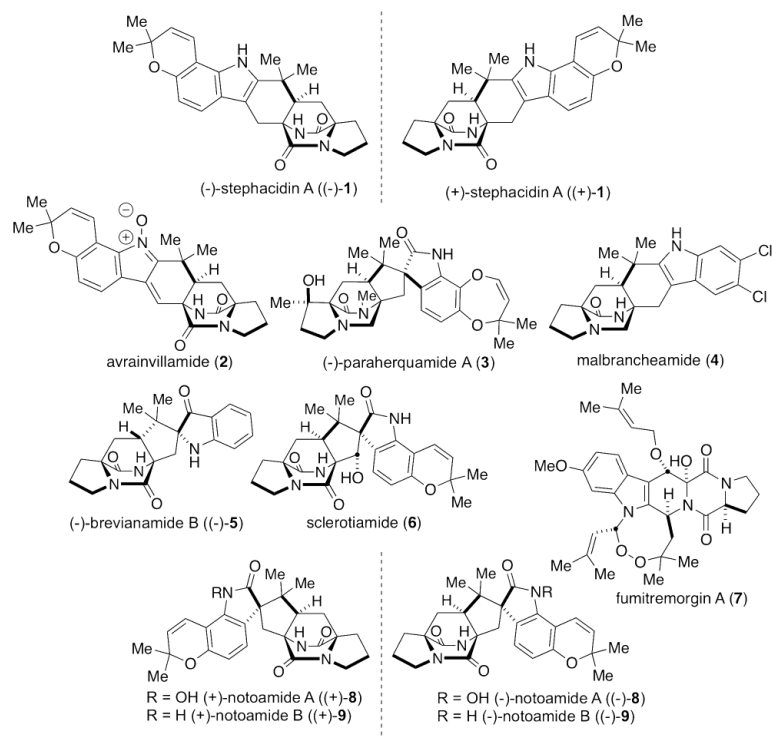
Figure 1.
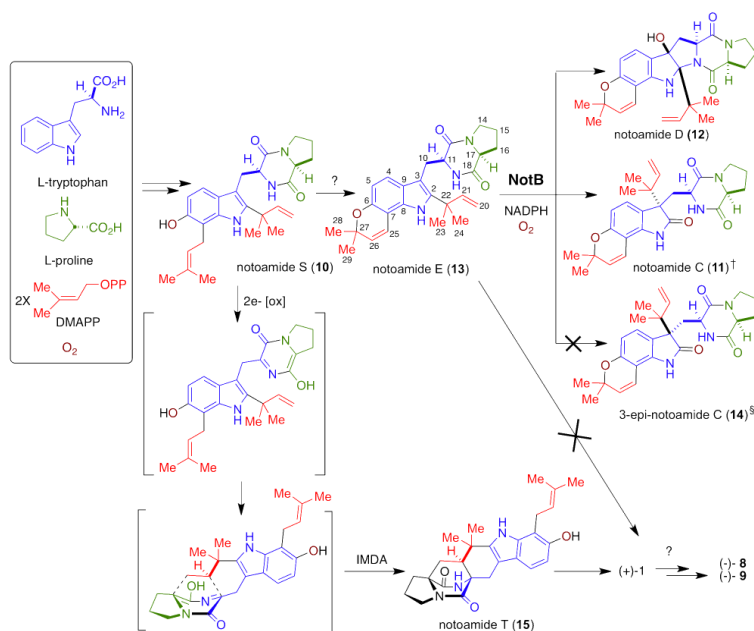Representative fungal prenylated indole alkaloids.

Figure 2.
Putative biosynthetic pathway for stephacidin and the notoamides. Structures of **11**[†] and **14**[§] are revised based on results of this study (see Supporting Information).
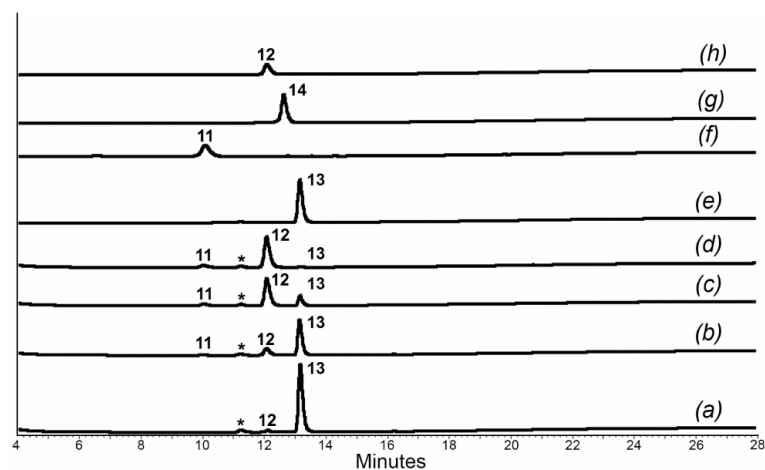
Figure 3.
HPLC analysis (240 nm) of *in vitro* NotB reaction using notoamide E (**13**) as substrate. The 100 μL reaction containing 1 μM NotB, 200 μM **13**, and 2.5 mM NADPH was performed at 28 °C for 1 min (a), 5 min (b), 15 min (c), and 50 min (d). Traces (e)-(h) showed analysis of authentic standards of **13, 11, 14**, and **12**, respectively. The asterisks denote a minor artifact from reaction mixture.
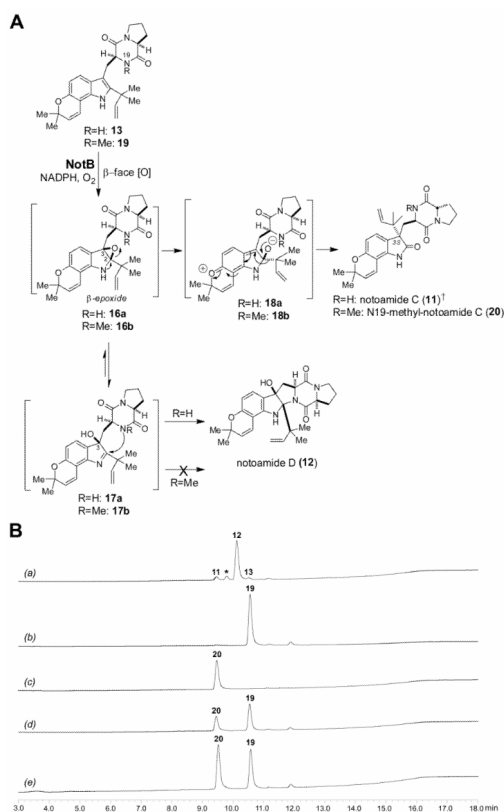
Figure 4.
(A) New presumed mechanism for NotB based on its catalytic activity against **13** and **19**. The revised structure of **11**[†] is shown. (B) HPLC analysis of *in vitro* NotB reaction (10 h) using **19** as substrate. (a) NotB + **13**; (b) authentic standard of **19**; (c) authentic standard of **20**; (d) *notB* + **19**; (e) sample (d) co-injected with authentic **20**. The asterisk denotes an artifact in the reaction mixture.